

# Measurement of tensor polarization in elastic electron-deuteron scattering

K. Hafidi <sup>a\*</sup>

<sup>a</sup>DAPNIA-SPhN, CEA/Saclay,  
91191 Gif-sur-Yvette, France

The tensor polarization observables ( $t_{20}$ ,  $t_{21}$  and  $t_{22}$ ) of recoil deuterons have been measured in elastic electron-deuteron scattering for six values of momentum transfer between 4.1 and 6.7 fm<sup>-1</sup>. The experiment was performed at the Jefferson Laboratory, using the electron HMS spectrometer, a deuteron magnetic channel and the polarimeter POLDER. The available range of polarization data has been considerably extended, allowing the determination of the charge form factors  $G_C$  and  $G_Q$  in the region of the secondary maximum of  $|G_C|$ .

## 1. The experiment

The deuteron electromagnetic form factors provide important tests of the nucleon-nucleon interaction and of a variety of nuclear models. Their determination up to momentum transfer  $Q$  comparable to the inverse of the nucleon core size probes the influence of non-nucleonic degrees of freedom and of relativistic effects in nuclei.

Measurements of the elastic electron-deuteron cross-section yield the structure functions  $A$  and  $B$ , related to the three form factors of the deuteron ( $G_C$ ,  $G_Q$  and  $G_M$ ) through

$$S(Q, \theta_e) = G_C^2(Q) + \frac{8}{9}\eta^2 G_Q^2(Q) + \frac{2}{3}\eta\varepsilon(Q, \theta_e)^{-1} G_M^2(Q) \equiv A(Q) + B(Q) \tan^2 \frac{\theta_e}{2}, \quad (1)$$

with  $\eta = Q^2/4M_d^2$  and  $\varepsilon = [1 + 2(1 + \eta)\tan^2 \frac{\theta_e}{2}]^{-1}$  is the virtual photon longitudinal polarization. The separate determination of  $G_C$  and  $G_Q$  necessitates the additional measurement of at least one deuteron polarization observable. The observable of choice is

$$t_{20} = -\frac{1}{\sqrt{2} \cdot S} \left[ \frac{8}{3}\eta G_C G_Q + \frac{8}{9}\eta^2 G_Q^2 + \frac{1}{3}\eta\varepsilon^{-1} G_M^2 \right]. \quad (2)$$

The other tensor moments

$$t_{21} = \frac{2}{\sqrt{3} \cdot S} \eta \left( \eta + \eta^2 \sin^2 \frac{\theta_e}{2} \right)^{1/2} G_M G_Q \sec \frac{\theta_e}{2} \quad \text{and} \quad t_{22} = -\frac{1}{2\sqrt{3} \cdot S} \eta G_M^2 \quad (3)$$

were measured as well. For comparison with other experiments or with theoretical models, small corrections of order  $B/A$  and  $B \tan^2 \frac{\theta_e}{2}/A$  are applied to the measured  $t_{2j}(Q, \theta_e)$  to get  $\tilde{t}_{20} \equiv t_{20}(G_M = 0)$  and  $t_{2j}(\theta_e = 70^\circ)$ .

The experiment was performed in the Hall C of the Jefferson Laboratory. Using a 120  $\mu$ A electron beam on a 12 cm long liquid deuterium target, the scattered electrons

---

\*Representing the Jefferson Lab  $t_{20}$  collaboration: see <http://t20.jlab.org> for a complete list of authors.

were detected in the HMS spectrometer, while the recoil deuterons were focussed in a specially designed magnetic channel onto the polarimeter POLDER [1]. The  $ed$  events were identified unambiguously through the HMS momentum, the coincidence time and the ADC signals from the POLDER front scintillators. In the POLDER liquid hydrogen target, a fraction of the deuterons from  $ed$  events underwent a charge exchange reaction  $p(d, pp)n$  which is sensitive to their tensor polarization. This fraction, also called efficiency, is of the order of  $3\text{-}6 \times 10^{-3}$ . The two protons from the charge exchange reaction were detected in small relative angle configurations with scintillator hodoscopes. POLDER was calibrated at the synchrotron SATURNE with polarized deuteron beams, so that the unpolarized efficiencies and analyzing powers of the  $p(d, pp)n$  reaction are known for deuteron energies between 160 and 520 MeV.

The efficiencies during the Jefferson Lab experiment and the calibration were compared to extract  $t_{20}$ . Two different proton tracking algorithms were used, yielding slightly different efficiencies, but same ratios of efficiencies when comparing experiment and calibration, and thus the same results for  $t_{20}$ . The control of efficiencies to a level of about 0.6%, combined with other sources of errors, results in quite small systematic errors in  $t_{20}$ , of the order of 0.05, except for the points at  $Q = 4.1$  and  $6.2 \text{ fm}^{-1}$ . The point at  $Q = 4.1 \text{ fm}^{-1}$  corresponds to low deuteron energies where the polarimeter response exhibits a marked energy dependence. The statistical errors vary from 0.03 to 0.18 from low to high  $Q$  values. The other tensor moments  $t_{21}$  and  $t_{22}$  are deduced from the azimuthal distribution of the proton pairs: unlike  $t_{20}$ , they are insensitive on the absolute normalization of the efficiencies.  $t_{21}$  is however more sensitive to detector alignment and to software cuts defining a cylindrical acceptance of the proton pair for each event.

## 2. Results and interpretation

Close to final results for  $\tilde{t}_{20}$ ,  $t_{21}(70^\circ)$  and  $t_{22}$  are presented in Fig. 1, and compared with the existing world data and with some recent theoretical calculations. When the new data overlap with the earlier one from Bates [2], they agree within the combined uncertainties, although our  $\tilde{t}_{20}$  points lie systematically higher. The indication of zero-crossing of  $t_{21}$  confirms the existence of a minimum in  $B(Q)$ .

In the same experiment, though with specific conditions (smaller deuterium target and electron solid angle), the structure function  $A(Q)$  was also measured [3]. Two different combinations of  $G_C$  and  $G_Q$  can be solved [14] to yield the results given in Fig. 2. The passage of  $G_C$  through 0 and to negative values is clearly seen.

In the non relativistic calculation of the deuteron form factors from  $np$  potentials, the perturbative addition of isoscalar meson exchange currents is mandatory to yield a better agreement with our data [7,8]. Differences coming from the nature of the MEC terms considered, as well as from meson-nucleon vertices, the  $\rho\pi\gamma$  coupling constant and the elementary nucleon form factors, still need to be sorted out and different  $np$  potentials should be compared (Paris, Argonne  $v18$ , Nijmegen, Bonn CD, etc) - see ref. [9].

Relativistic models have been refined in the past few years, whether in various 3-D reductions of the Bethe-Salpeter equation [10,11] or in Light-Front Dynamics [12,13]. These models give a very good description of our data. In the later, the inclusion of  $\rho\pi\gamma$  and recoil MEC terms is being implemented [14].

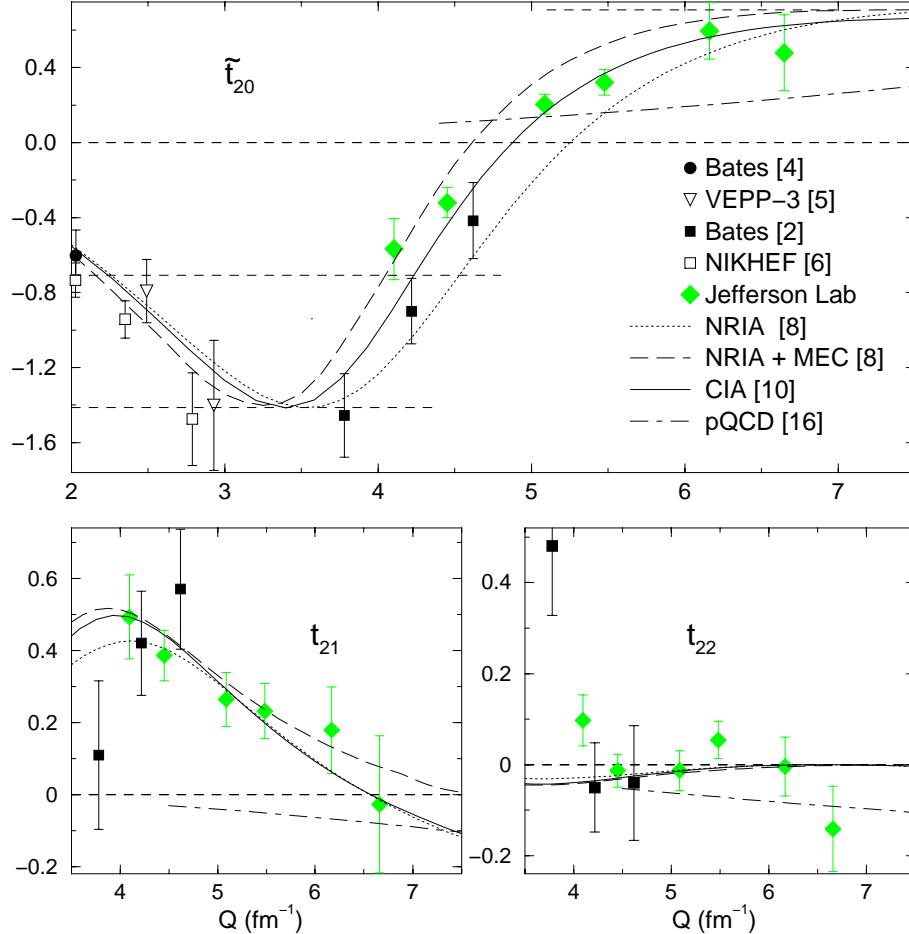


Figure 1.  $\tilde{t}_{20}$ ,  $t_{21}$  and  $t_{22}$ : experiments and some theoretical models. Horizontal dashed lines correspond to specific values of  $\tilde{t}_{20}$ :  $-\sqrt{2}$ ,  $-1/\sqrt{2}$  ( $G_C = 0$ ), 0 and  $+1/\sqrt{2}$ .

Quark degrees of freedom in the deuteron wave function have been considered in [15] and previous work. Unfortunately, the impulse approximation has not been constructed in a consistent way in [15], but the size of conventional MEC as well as additional contributions due to quark exchange is compatible with what can be inferred from our data.

Finally, perturbative QCD predicts the dominance of the transition between deuteron zero helicity states in the initial and final states at high  $Q$  [16]. From this hypothesis, ratios such as  $B/A$  and  $t_{ij}$  can be calculated, but differ from experiment in the region of momentum transfers considered here. Even the relative sign of  $G_M$  and  $G_Q$  is wrong in this hypothesis (see the  $t_{21}$  results). It can be shown indeed that the double helicity flip transition is at least as large as the  $0 \rightarrow 0$  transition in this  $Q$ -range [17].

### 3. Conclusion

We have measured  $t_{20}$ ,  $t_{21}$  and  $t_{22}$  between 4.1 and 6.7  $\text{fm}^{-1}$  in elastic electron-deuteron scattering, with a precision often better than the existing data at lower  $Q$ . This data, together with our new data on the structure function  $A(Q)$ , provide a good determination of the deuteron charge and quadrupole form factors to the highest momentum transfers

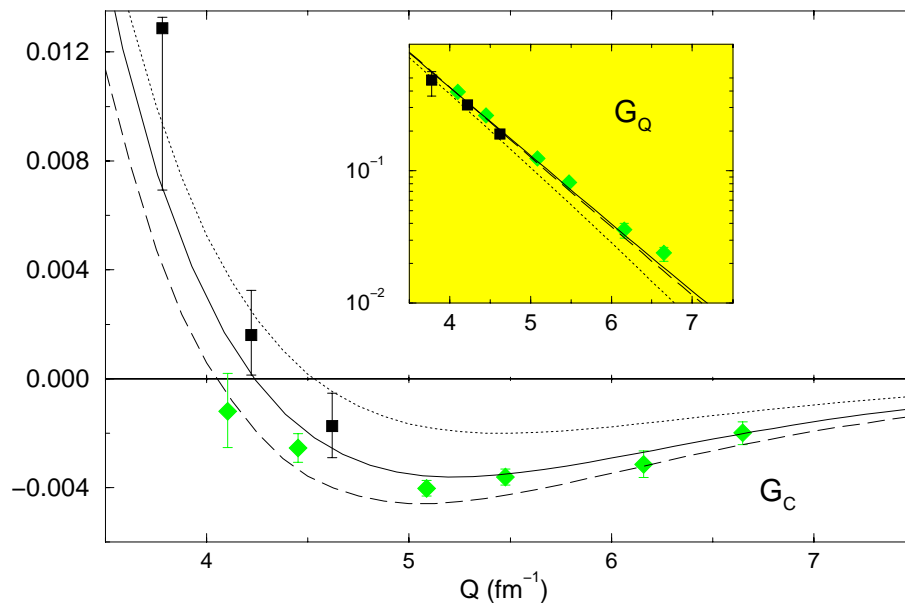


Figure 2. Deuteron monopole ( $G_C$ ) and quadrupole ( $G_Q$ ) form factors. See Fig. 1 for legend.

so far. All these observables put significant constraints on the exact determination of isoscalar meson exchange currents and are in favor of fully relativistic calculations. Complementary measurements between 3 and 4.5  $\text{fm}^{-1}$  are expected from internal polarized targets at VEPP-3 and Bates, for a still better determination of the node of  $G_C$ .

## REFERENCES

1. S. Kox *et al.* Nucl. Instr. Meth. **A346**, 527 (1994); L. Eyraud, Thesis, University Joseph Fourier, Grenoble (1998).
2. M. Garçon *et al.*, Phys. Rev. C **49**, 2516 (1994).
3. D. Abbott *et al.*, Phys. Rev. Lett. **82**, 1379 (1999).
4. M.E. Schulze *et al.*, Phys. Rev. Lett. **52**, 597 (1984).
5. R. Gilman *et al.*, Phys. Rev. Lett. **65**, 1733 (1990).
6. M. Bouwuis *et al.*, Phys. Rev. Lett. **82**, 3755 (1999).
7. B. Mosconi and P. Ricci, Few-Body Syst. **6**, 63 (1989); **8**, 159(E) (1990).
8. R.B. Wiringa *et al.*, Phys. Rev. C **51**, 38 (1995).
9. W. Plessas *et al.*, Few-Body Syst. Suppl. **9**, 429 (1995).
10. J.W. Van Orden *et al.*, Phys. Rev. Lett. **75**, 4369 (1995).
11. D.R. Phillips *et al.*, Phys. Rev. C **58**, 2261 (1998).
12. J. Carbonell *et al.*, Phys. Rep. **300**, 215 (1998).
13. V. Karmanov, Proc. this conference.
14. K. Hafidi, Thesis, University of Paris-Sud, Orsay (1999).
15. A. Buchmann *et al.*, Nucl. Phys. **A496**, 621 (1989).
16. S.J. Brodsky and J.R. Hiller, Phys. Rev. D **46**, 2141 (1992).
17. M. Garçon *et al.*, Proc. Int. Nucl. Phys. Conf. (INPC98), Paris.